

See discussions, stats, and author profiles for this publication at: <https://www.researchgate.net/publication/356355726>

Holocene Aridity-Induced Interruptions of Human Activity along a Fluvial Channel in Egypt's Northern Delta

Article in *Quaternary* · November 2021

DOI: 10.3390/quat4040039

CITATIONS

0

READS

89

3 authors:



Jean-Daniel Stanley

Smithsonian Institution

312 PUBLICATIONS 9,864 CITATIONS

[SEE PROFILE](#)



Tobias Ullmann

University of Wuerzburg

57 PUBLICATIONS 627 CITATIONS

[SEE PROFILE](#)



Eva Lange-Athinodorou

University of Wuerzburg

40 PUBLICATIONS 81 CITATIONS

[SEE PROFILE](#)

Some of the authors of this publication are also working on these related projects:




Comparing the performance of crop growth models using synthetic remote sensing data at DEMMIN, Germany [View project](#)



Archaeology and Geomorphology of the Nile Delta [View project](#)

Article

Holocene Aridity-Induced Interruptions of Human Activity along a Fluvial Channel in Egypt's Northern Delta

Jean-Daniel Stanley ^{1,*}, Tobias Ullmann ²  and Eva Lange-Athinodorou ³¹ Mediterranean Basin (MEDIBA) Program, 6814 Shenandoah Court, Adamstown, MD 21710, USA² Institute of Geography und Geology, Physical Geography, University of Würzburg, 97074 Würzburg, Germany; tobias.ullmann@uni-wuerzburg.de³ Institute of Egyptology, University of Würzburg, 97070 Würzburg, Germany; eva.lange@uni-wuerzburg.de

* Correspondence: stanleyjd0@gmail.com

Abstract: Gearchaeological information presented here pertains to a subsidiary Nile channel that once flowed west of the main Sebennitic distributary and discharged its water and sediments at Egypt's then north-central deltaic coast. Periodical paleoclimatic episodes during the later Middle and Upper Holocene included decreased rainfall and increased aridity that reduced the Nile's flow levels and thus likely disrupted nautical transport and anthropogenic activity along this channel. Such changes in this deltaic sector, positioned adjacent to the Levantine Basin in the Eastern Mediterranean, can be attributed to climatic shifts triggered as far as the North Atlantic to the west, and African highland source areas of the Egyptian Nile to the south. Of special interest in a study core recovered along the channel are several sediment sequences without anthropogenic material that are interbedded between strata comprising numerous potsherds. The former are interpreted here as markers of increased regional aridity and reduced Nile flow which could have periodically disrupted the regional distribution of goods and nautical activities. Such times occurred ~5000 years B.P., ~4200–4000 years B.P., ~3200–2800 years B.P., ~2300–2200 years B.P., and more recently. Periods comparable to these are also identified by altered proportions of pollen, isotopic and compositional components in different radiocarbon-dated Holocene cores recovered elsewhere in the Nile delta, the Levantine region to the east and north of Egypt, and in the Faiyum depression south of the delta.

Keywords: Nile delta; Sebennitic; paleoenvironment; paleoclimate; Nile flow; ge archaeology

check for updates

Citation: Stanley, J.-D.; Ullmann, T.; Lange-Athinodorou, E. Holocene Aridity-Induced Interruptions of Human Activity along a Fluvial Channel in Egypt's Northern Delta. *Quaternary* **2021**, *4*, 39. <https://doi.org/10.3390/quat4040039>

Academic Editors: David Bridgland, Xianyan Wang and Jef Vandenberghe

Received: 15 September 2021

Accepted: 12 November 2021

Published: 18 November 2021

Publisher's Note: MDPI stays neutral with regard to jurisdictional claims in published maps and institutional affiliations.



Copyright: © 2021 by the authors. Licensee MDPI, Basel, Switzerland. This article is an open access article distributed under the terms and conditions of the Creative Commons Attribution (CC BY) license (<https://creativecommons.org/licenses/by/4.0/>).

1. Introduction

Herodotus, in his "Histories" [1], compiled in the mid-5th century B.C., identified five active river branches that reached the Nile delta coast at the time of his visit to Egypt, several of which are now extinct. He recognized the Sebennitic as one of these, and referring to its then still active channel noted (Book 2, Chapter 17.4): "This is by no means where the least share of [the Nile's] water flows, nor is it [the Sebennitic] the least famous." Its water reached the delta's southern apex and, from there, cleaved the delta in two as it migrated northward to the coast. The Sebennitic continued to funnel Nile water toward that region until about 800 to 1000 AD [2,3], after which flow was diverted from its north-trending path via other distributaries toward more NE and NW deltaic sectors [4,5].

One of the numerous drill cores recovered from east to west across the northern Nile delta by the Smithsonian Institution attracted special attention 30 years ago [6]. Identified as S-44, it was positioned along a subsequent, somewhat younger channel to the west of the major Sebennitic distributary which flowed northward to the coast along what is presently the eastern margin of Burullus lagoon (Figure 1).

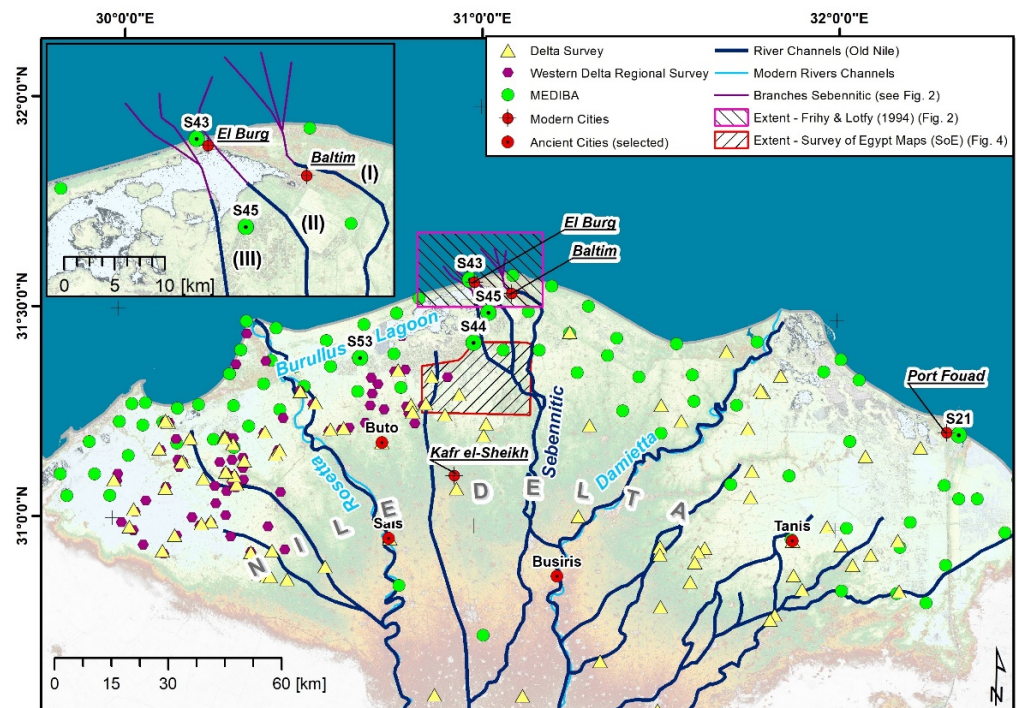


Figure 1. Map of the Nile delta showing former Sebennitic distributary and present Rosetta and Damietta channels. Areas cited in the article are shown, including core locations of the MEDIBA project, and archaeological sites as indicated by the “Delta Survey” and the “Western Regional Delta Survey” of the Egypt Exploration Society. Background map draws the digital elevation model of the TanDEM-X Mission. TanDEM-X DEM courtesy of the German Aerospace Center (© DLR).

Its content was unique with respect to two attributes in cores that had until then been discovered in the northernmost delta: it comprised an unusually large amount of pottery, and among these were the oldest yet found in the northernmost central delta, dated to the New Kingdom. These, and potsherds of the Late Period and Ptolemaic Period, were concentrated in three separate layers, each of which was younger as one progressed up-core. Previous studies [6,7] focused on potsherd-rich deposits with which to date the Holocene section and record the timing and importance of human activity along this sub-branch channel in a region where much remains to be discovered.

The present study now explores a different aspect, focusing primarily on the possible origin and significance of interbedded Holocene sediment strata in core S-44 that are without human-introduced material. This approach could shed new information with which to better interpret the depositional origin and the evolving anthropogenic history in this deltaic sector. While not obvious at the time of the original survey, a series of findings made during past decades can now help explain why the presence of sediment layers without anthropogenic material in the study core probably did not accumulate randomly time-wise. This absence of material can presently be more reliably interpreted by taking into account dated Holocene environmental events, particularly paleoclimatic ones. These periodic episodes during the time of channel deposition would likely have affected human activity in this study sector.

2. Materials and Methods

2.1. Paleogeographic Setting of Study Area

While no longer active in the northernmost sector of the delta, the Nile’s major Sebennitic branch once flowed to a north-central coastal area positioned almost midway between where the younger Rosetta and Damietta distributaries presently reach the Mediterranean (Figure 1). The Sebennitic distributary’s considerable volume of water and sediment were

once dispersed at the coast and onto the continental shelf seaward of where the central delta at the time formed a large fluvial-derived promontory (cf. [4,8]). What presently still remains of this former more angular, seaward-trending Sebennitic feature [7,9] is now a broad, curved arcuate, intensely wave-eroded coastline [10], the so-called north-central deltaic Burullus bulge (Figure 1).

Of special interest here is core S-44, recovered along a former subsidiary channel positioned ca. 10 km to the west of the major Sebennitic distributary (Figure 1) that had once also flowed northward, distributing water and sediment to the coast and shelf beyond. The eastern part of Burullus lagoon presently covers much of this former channel. This water body is the second largest in the northern delta, with a configuration and area that has been considerably modified during the Holocene to the present [11,12]. Water and sediments flowing in the smaller subsidiary channel were once dispersed to and beyond the coast in a sector mostly to the west of the deposits released offshore earlier by the main Sebennitic distributary. Offshore current-reworked deposits of both channels appear as three broad and partially superposed arcuate sectors (Figure 2) formed in part by sand, silty sand, and sandy silt [13]. The largest earlier one (coded as I, in large part of Lower to Middle Holocene age) is defined by the configuration of the 18 m isobath to the north and east, and is partially superposed to the west by the subsequent two smaller arcuate ones (coded as II, of Lower to Middle Holocene, and III, primarily discussed herein, of largely Upper Holocene age) defined by the 16 and 14 m isobaths (Figure 2). Channel III is located west of the major Sebennitic distributaries I and II (Figure 1). These seafloor features highlight the partial burial of the earlier major distributary channel deposits by those of the younger, subsequent migrating channels that in time were released north of the Burullus outlet. A somewhat similar pattern of offshore displaced coarser-grained deposits is also depicted on charts offshore the Nile delta ([3] Figures II/48, IV/1, and IX/10). Depositional histories are also recorded along the delta's margin by the present markedly wave-eroded shoreline [10,14], bordered by an extensive belt of sand-rich coastal ridges and broad, widespread dune fields. These are readily apparent on land photographs [15,16] and satellite images [12,17–19]. This investigation also takes into account litho- and chronostratigraphic, sedimentological, and biogenic findings revealed by 22 drill cores (S-38 to S-59) along the northern delta land margin where the average thickness of the Holocene section is 13.5 m [20].

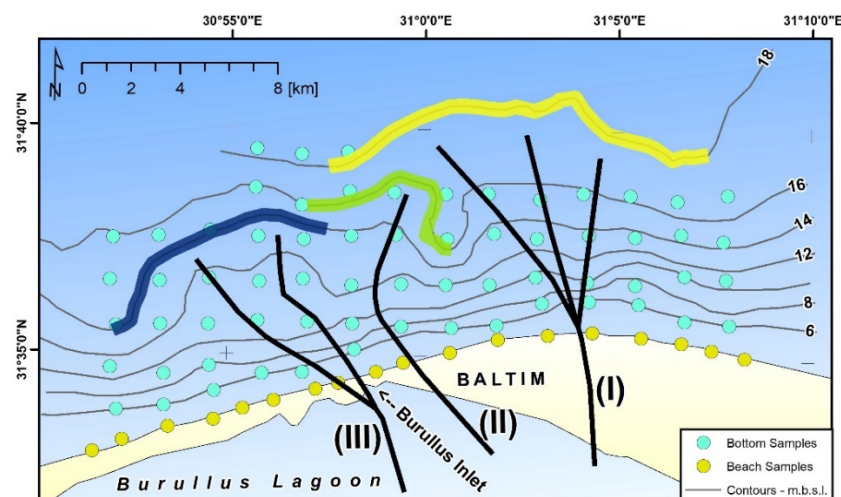


Figure 2. Map of Nile delta coastal margin showing water depths from the coast to the present current-eroded arcuate Burullus bulge. The position highlighted in yellow of the Nile's early major Sebennitic discharge (I) to 18 m depths; then its position after having shifted toward the west (II), in green, at about the 16 m isobath, and that of the subsequent smaller subsidiary channel deposits in blue at the 14 m isobath (III) of prime focus in this study. Seafloor bathymetry and sample sites serving as the base are after [13].

Of these, three cores in particular (S-44, S-45, and S-43; in Figure 1), recovered from south to north to the present coast (Figure 1), outline the former regional paleogeography and shed light on past environmental conditions in the study area [6,7,11]. These borings record the presence of an underlying channel fill buried by fluvial sands and sandy silt with interbedded silt and mud, some likely derived from the channel's adjacent margins. Sand layers were deposited beneath lagoonal silty muds, and younger overlying coastal sands that generally cover older deposits at the delta margin ([11], their Figure 9).

Major Sebennitic flow had reached the coast in proximity to the northernmost center of the Burullus bulge by Lower Holocene time to the Middle Holocene, and may have continued there until, or somewhat after, the late Middle Holocene and perhaps at/or after ~5000–4500 years B.P. Butzer (2002, p. 90) [21] reviewed five phases of Nile flows through Holocene time. He notes that his phase 5 “marks the inauguration of the ‘modern’ fluvial regime [. . .] since New Kingdom times” with flood energy for the most part lower than during the previous Middle Holocene to about 2000 years B.C. This is recorded by a progressive atrophy of five of the traditional Nile branches between 3000 and 2000 years ago, as also found in this present study area. In time, a channel deflection may have been triggered by the thick and extensive accumulations of near-coastal deposits that had formed a partial barrier blocking some of the distributary's northern coastal margin outflow. These sediments were then reworked by wind and coastal currents, thus reshaping the delta's promontory into a broad arcuate Burullus coastal bulge [10]. It is likely that some of these coastal margins and offshore deposits were also shifted by other physical interventions: rise in sea level [22–25], land subsidence [26], compaction of underlying deposits [27], neotectonic displacement, and lowering [28–30]. A progressive overall lowering of land relative to sea level in this northern region at a rate of 7.7 mm per year is attributed to the interplay of these diverse factors [26].

2.2. Topographic Maps and Satellite Imagery

For further information on the hydrographic and topographic setting at S-44, several map sheets of the Survey of Egypt (SoE) were analyzed. These topographic maps were recorded in the 1930s and include elevation above sea-level measurements from land surveying as point features. In total, four sheets (96/615, 96/600, 95/600, and 95/615) of this map series at a scale of 1:25,000 were available (through Dr. Robert Schiestl of the LMU Munich, see Acknowledgments). These sufficiently covered the site S-44 and its surroundings (approx. 30 km by 20 km); however, no map sheets north (towards Baltim) of S-44 were available.

Using a GIS-based approach, the SoE maps were further processed to overlay the topographic information with the results of the above-mentioned surveys (Figure 1) and to compare the topographic and hydrographic information in relation to findings of the S-44 records. The following steps, schematically illustrated in Figure 3, were conducted to extract a digital elevation model (DEM) from the SoE data (cf. [19,31], who conducted similar analyses of SoE maps): (1) The map sheets were georeferenced in ArcMap (Version 10.6) using the inherent information on the geolocation (i.e., the provided coordinates). The geocoded map sheets were then cropped and mosaicked to a single file (Figure 3a). (2) Data on the elevation above sea level were digitized (Figure 3b). This included the digitalization of the contour lines with one-meter equidistance (generating ca. 240 line features) and of the land survey points, generating ca. 2700 points indicating the land elevation with a point density of approx. 9 points per km². Besides, the locations labeled as “Ruins” in the SoE maps were digitized and stored as point features. (3) Using the point data on the land elevation, the Natural Neighbor algorithm was used in ArcMap to convert the point information to a digital elevation model (DEM) with 80 m by 80 m pixel spacing (raster format) (Figure 3c). (4) This DEM was further processed in the software SAGA GIS Version 7 (<http://www.saga-gis.org>, accessed on 8 September 2021) and hydrographic modeling was conducted [32]. The aim of this modeling was to identify remains and landforms related to past fluvial activity, such as levees.

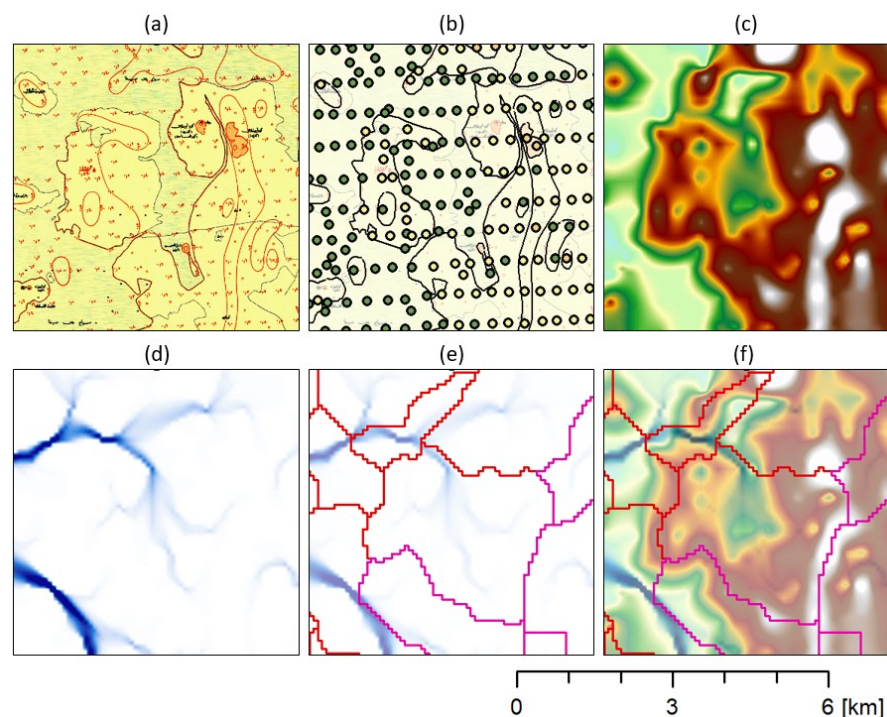


Figure 3. Simplified workflow illustrating the hydrographic modeling using digitized topographic maps of the Survey of Egypt (SoE). (a) SoE topographic maps, (b) digitized points showing land elevation above sea level, (c) interpolated digital elevation model (DEM), (d) multi-flow-direction flow accumulation (MFD), (e) delineated minor (red lines) and major (violet lines) basin boundaries, and (f) overlay of DEM, MFD, and basin boundaries.

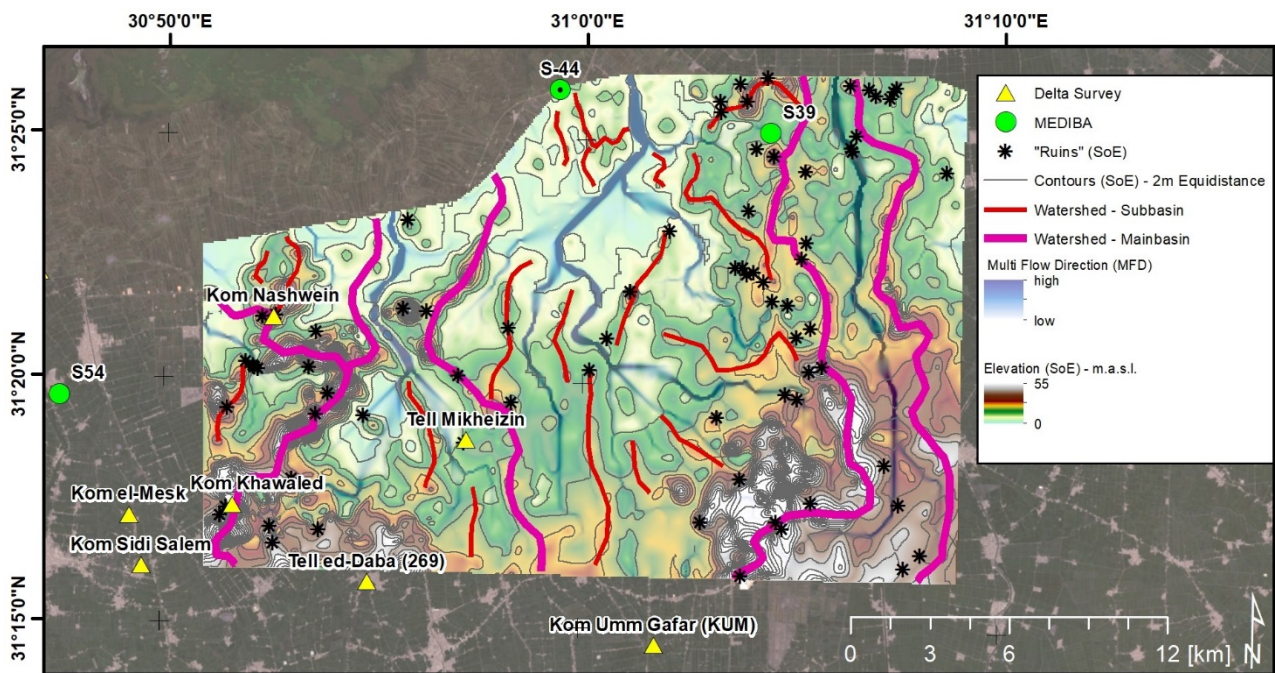
The DEM was preprocessed using the filling approach of [33] with a minimum slope of 0.001. Further processing included the calculation of the *deterministic-eight* flow direction (D8) and the *multi-flow direction* (MFD) flow accumulation (Figure 3d). The processing of minor and major basin boundaries was realized using the extend watershed tool (Figure 3e). These basin boundaries were visually inspected and line segments coinciding with higher elevated ground (with respect to the DEM) were extracted. This was done as basin boundaries were artificially/randomly created over regions without significant topography; as such, the most meaningful line segments, most likely indicating the above-mentioned levees, were selected. (5) Finally, the DEM, MFD, and the selected minor and major basin boundaries were overlaid and compiled as a map (Figure 3f).

Further auxiliary information included recent satellite imagery from Sentinel-2, acquired in 2020 and accessed via the Sentinel Open Access Hub (<https://scihub.copernicus.eu> (accessed on 26 April 2021)) and archive data of declassified CORONA imagery, acquired in 1968 and accessed via the “CORONA Atlas of the Middle East” (<https://corona.cast.uark.edu> (accessed on 20 April 2021)). Both datasets were integrated into the geodatabase and compared to and with the results of the hydrographic modeling.

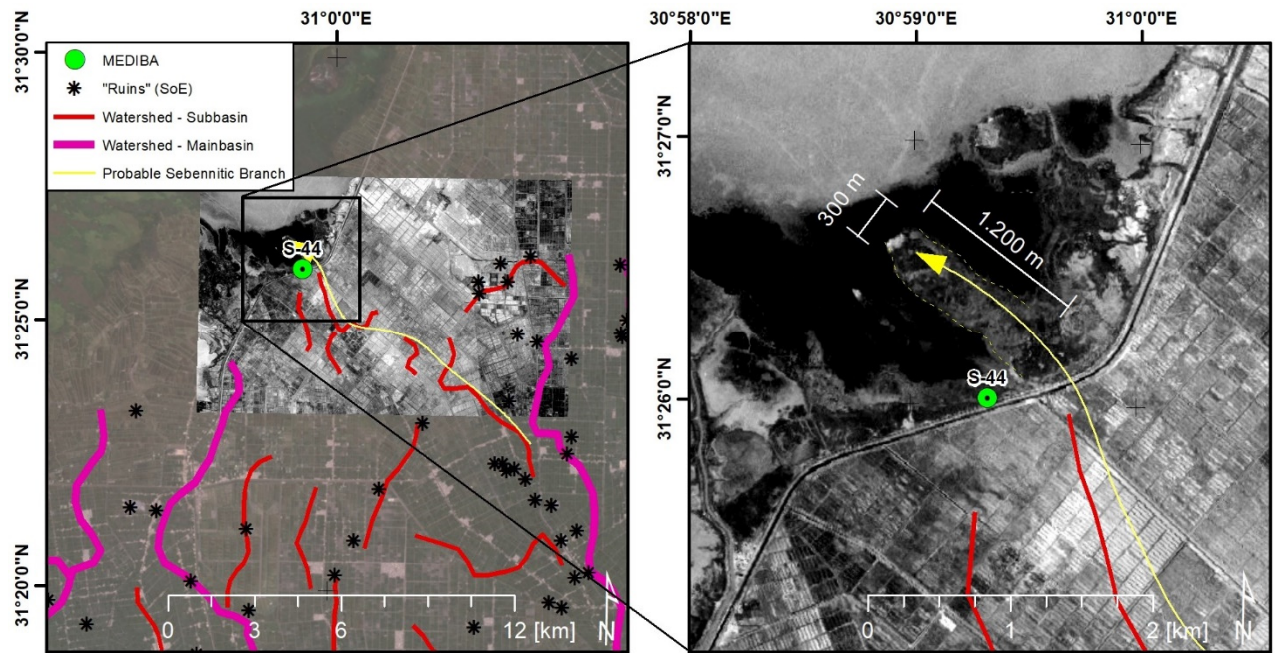
3. Results

3.1. Satellite Imagery, Topographic Maps, and Hydrographic Modeling

Hydrographic analyses of the DEM derived from the SoE maps indicate two smaller more recent Sebennitic channels as defined by two parallel red lines (minor basin boundaries) that trend SE of the S-44 site (Figure 4a). The subsidiary channel appears to have been bordered by a levee whose upper surface is presently above the lagoon’s water level at present, which is revealed by the CORONA imagery (Figure 4b). No distinct remains of an ancient settlement have yet been discovered on the surface of, or close to, this feature, nor is there any information in the SoE maps of the CORONA or Sentinel-2 imagery.



(a)



(b)

(c)

Figure 4. (a) Maps of the results of the hydrography modeling using elevation information digitized from the topographic maps of the Survey of Egypt (SoE 1:25 k series) and archaeological sites of the “Delta Survey” of the Egypt Exploration Society (<https://www.ees.ac.uk/delta-survey>, (accessed 7 April 2021)). Lower Panel: Corona Imagery (acquired in 1968) from the “CORONA Atlas of the Middle East” of site S-44. (b) Corona imagery, results of the hydrography modeling using elevation information digitized from the topographic maps of the Survey of Egypt (SoE. 1:25k series) and locations of “Ruins” (indicated in the SoE maps). (c) Land surface details at site S-44 and indications/annotations on a probable former levee stretching NW of S-44. The background image in the left panel shows a recent true-color satellite image of Sentinel-2 acquired in June 2020, and the potential flow path of the subsidiary Sebennitic branch (yellow arrow in panels in (b,c)).

However, related work reports Ptolemaic and Roman pottery and other vestiges are found on a number of elevated sectors examined in this general eastern Burullus lagoon

area [34,35]. The possibility of discovering an once-existing settlement in the vicinity of S-44 is thus not excluded until more closely spaced exploratory deep drilling and archaeological subsurface surveys and excavations are made in close proximity to the study site. It is proposed, for the time being, that the area adjoining the potsherd-rich channel site may have contained a base for a trade facility, possibly a harbor, in a sector that could periodically have been used for the exchange and distribution of goods transported by boat at various times between the New Kingdom and Ptolemaic periods. Interestingly, although we do not have archaeological remains to further corroborate this scenario, a textual source from the time of the Old Kingdom (4th dynasty, c. 2600 BC) mentions a location with the name “new (river) mouth” which might refer to a harbor or settlement close to a river estuary of the Sebennitic branch in the northern central delta, as the context of the text suggests [36]. The same source reveals the name of another location (“The great (river) mouth of the papyrus marshes”) for which further textual evidence points to a location in the Sebennitic area, and, judging from the name, could also refer to a settlement close to where the Sebennitic branch discharged in the Mediterranean Sea. Needless to say, this does not mean that the location of S-44 should be identified with either one of these, but it underlines the strong possibility of the existence of ancient settlements and/or harbors in that area.

Results of the hydrographic modeling further indicate two possible narrow width fluvial-like features that extend across the north-central delta area, and appear to have reached, and possibly joined together, at or near the S-44 site (Figure 4a). One of these extends in a northwesterly direction from a sector originally positioned ca. ~14 km distant to the southeast, possibly joining the former larger Sebennitic distributary channel, which is indicated as the mainbasin boundary by the hydrographic modeling (NE of Kom Umm Gafar (Figure 4a)). The other trends N-NE from a more central deltaic sector, one that perhaps could have included Nile flow passing near one or more larger archaeological sites south of Burullus lagoon, such as Tell Mikheizin, Tell ed-Daba, or Kom Kahwaled (at least as noted in Figure 4a). These two fluvial trends may also follow what appears to be more recently emplaced artificial drains (i.e., flow pathways on, or adjacent to, much older former natural low-elevation Nile channels). These can now collect and redirect wastewater from human settlements, and also from agricultural and fish farming centers, and away from this region for their discharge elsewhere [17,37,38].

3.2. Archaeological Record in Core S-44

The previous study of core S-44 provided a framework with which to determine the chronostratigraphic distribution of its Holocene pottery sherds. Included are some of the oldest anthropogenic materials yet discovered in the northern delta. The core site was recovered ~17 km due south of the Burullus lagoon’s outlet near El Burg village at the coast and ~16 km southwest of the town of Baltim (Figure 1). The site is positioned ~10 km west of the Nile’s former major north-trending Sebennitic distributary flow path, and ca. 35 km to the north of Xoïs, an early archaeological site, much of which remains buried and poorly defined, near the town of Kafr el-Sheikh in the mid-central delta. According to written sources, it dates back to the 3rd Millennium B.C. [39] but has not yet revealed structures older than the Ptolemaic period (2nd century A.D.; [40]).

The lower sections of cores recovered around Burullus lagoon by the Smithsonian Institution all recovered Late Pleistocene deposits, providing a chronostratigraphic baseline allowing us to focus on Holocene sediment sequences in the present study area [9,11,20]. S-44 is 21.4 m long, and its top lies at an elevation of ~1 m above present msl. Its lower ~7 m section is dated Upper Pleistocene, and the upper ~14 m section above it is late Middle to Upper Holocene (ca. 7000 years B.P. to present). The Late Pleistocene to late Middle Holocene floodplain comprises sandy silt and silty mud deposits. The litho-stratigraphic log of the Upper Holocene section records the following (Figure 5a): silty mud from the base upward (~14–9 m), organic-rich mud (~9–6 m), silty mud and rippled silty mud (~5.75–4.25 m), organic-rich mud (~4.25–1.5 m), and by silty mud in the uppermost 1.5 m

core section. Shell fragments, occurring primarily in sections from ~10.8 to 6 m and at the core top, record organisms requiring a wide range of salinity habitats that range from marine to brackish and freshwater. Up-core through time the sections record fluvial, lagoon margin, lagoon, and protected bay environments. The major focus until now has been on the core's three separate ceramic assemblages embedded in its Upper Holocene fluvial sediment section [6]. The lower and thickest sequence of sherds contains the most numerous and earliest pottery fragments in a layer about 3.5 m thick at a depth of ~9.5 m to ~6.0 m from the core top. The second separate sherd layer up-core was recovered at depths of ~4.7 to 4.5 m, and this was followed by the third separate layer at ~2.1 to 1.7 m near the core top.

It is of note that no anthropogenic materials were recorded in sediment sections at depths beneath ~9.5 m, between 6.0 m and 4.7 m, between 4.5 m and 2.1 m, and above 1.7 m (Figure 5a).

The 23 potsherds collected in the three distinct levels were sent for identification and dating to Dr. Dorothea Arnold and her archaeological staff at the Department of Egyptian Art at the Metropolitan Museum of Art in New York City. These materials ranged in size from 1.0 × 0.7 cm to 6.0 × 2.5 cm, are from 0.3 to 0.7 cm thick, and vary from angular to sub-rounded in shape. The majority of sherds are partially coated and range from brown to reddish-brown and yellowish-brown; one sampled at a depth of about 2 m has a black lustrous coating and was interpreted as Ptolemaic. Color photographs of selected sherds are featured in [6] (their Figures 6, 8, and 9 through 11). To minimize bias in attributing age and origin, each of the 23 fragments was shipped in a separate bag, and numerically coded non-sequentially by depth.

The code numbers and depths were retained and kept confidential at the Smithsonian until after completion of the identification process. The lower oldest and thickest sequence of sherds contained the most numerous ancient pottery fragments and were identified as New Kingdom age and dated from ~3600–3500 years B.P. to about ~3200–3000 years B.P. The next higher sherd layer up-core was of the Late Period age (~2700–2300 years B.P.). These two lower sequences were then followed near the core top by the third layer of largely Ptolemaic to early Roman age material (~2200–1800 years B.P.).

The potsherd ages at the S-44 site were determined primarily by archaeological methodology. X-radiographs that highlight the position of these fragments in the 8 cm diameter core sections made prior to sampling of sherd and sediment indicated these materials to be at or near their original in-situ position, with little to no obvious evidence of displacement by the drilling process. The physical attributes of these fragments suggest they were not likely displaced for a substantial distance in the channel by Nile flow to the core site but, rather, were collected at or near their site of introduction and final deposition.

The much larger size of dated sherds, the angularity and subangularity of some dated fragments, and remnants of coloration preserved on many of the potsherd surfaces and other attributes summarized above strongly suggest that these anthropogenic materials were not subject to extensive lateral movement, intense rubbing against each other, nor did they undergo substantial reduction and/or other evidence of erosive transport activity since their proximal deposition from the margin of the proximal fluvial channel as is indicated in the present study. In comparison with our multi-year projects involving the radiocarbon dating of Nile fluvio-deltaic sediments in the study area, and also elsewhere in the delta, we have recorded generally and more often than not radiocarbon ages of clay size, silt, and fine sand fractions of an older than expected age. Additionally, not infrequently older dated sediment strata in cores appear positioned above those of a younger age. Radiocarbon dating results provided in syntheses of some 400 or so dates from ~100 cores that ranged from 20 to 50 m in length collected across the northern delta reveal that the overall majority of these dated sedimentary materials have proved too old.

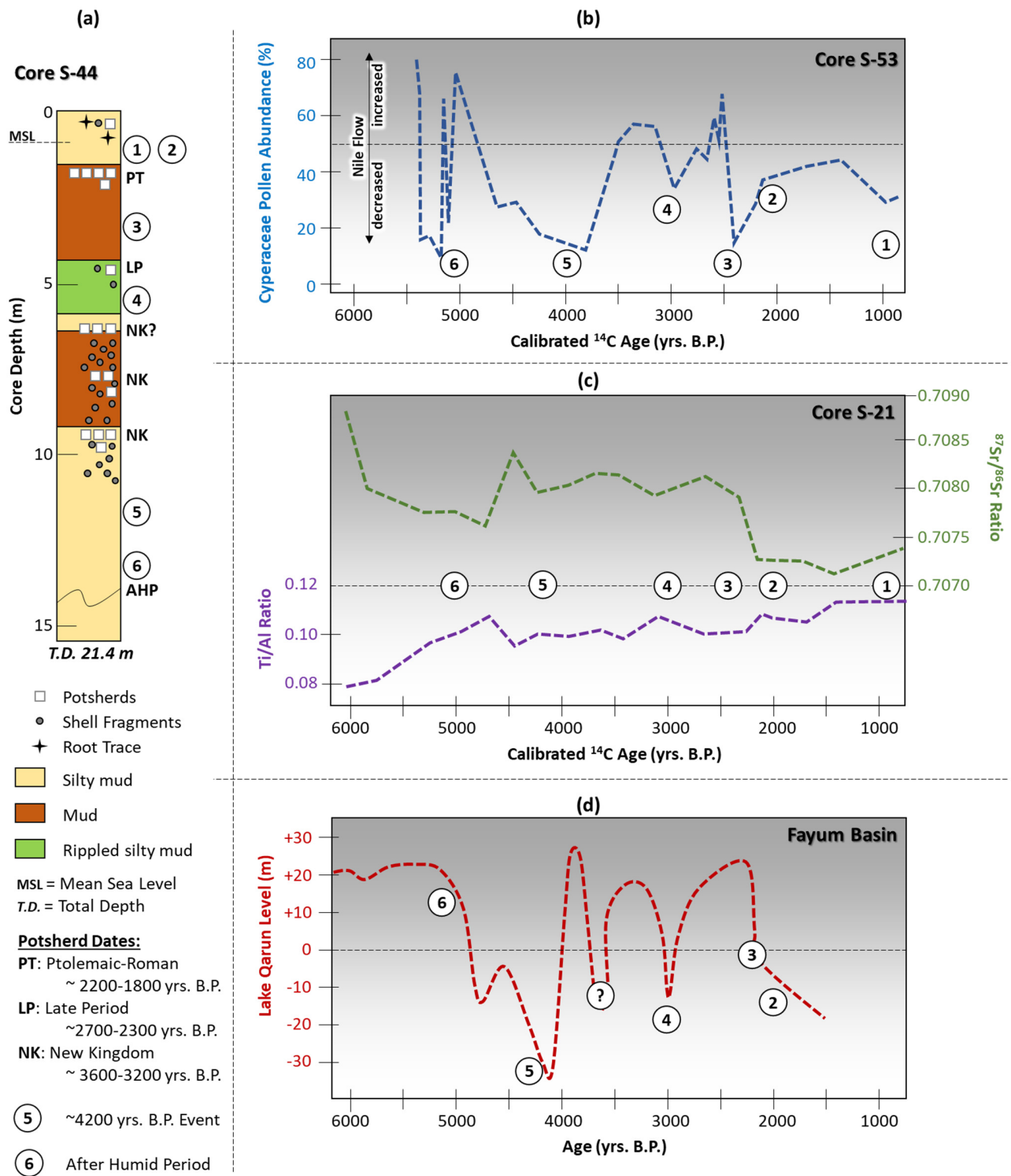


Figure 5. (a) Log of core S-44 recording its chrono- and litho-stratigraphy and position of dated potsherd-rich horizons (modified after [6]), and also layers without archaeological material. Circled numbers 1-6 refer to these latter deposits attributed herein to periods of increased aridification as defined in the text. Additionally shown, for comparison, are three additional radiocarbon-dated cores with sections also affected by aridification: (b) core 53, numbers 1-6, along the southwest margin of Burullus lagoon are based on Cyperaceae and other pollen abundances (modified after [41]); (c) core S-21 near Port Fouad along the NE delta coastal margin recording phases highlighted by Ti/Al and $^{87}\text{Sr}/^{86}\text{Sr}$ ratios (modified after [42]); (d) core collected in the Faiyum basin ~250 km south of the north-central delta coast recording estimated water levels in lake Qarun through time (modified after [43]). Calibrated ^{14}C dates in (b,c).

They commonly range in age anywhere from 100–200 yrs. to some as much as 1000 yrs., or well beyond a realistically expected time-span [20,44].

This scenario of commonly older-than-reasonably dated sediment is now attributed to being the result, at least in part, from the frequent reworking of some earlier deposited sediment fractions, commonly finer-grained ones, by mechanical displacement and their repeated erosion and re-depositional processes (“stop-and-go” transport) as noted in various fluvial-deltaic settings [44–46]. This mechanism can be envisioned where episodic fluvial intensities are periodically renewed and accompanied by erosional phases that erode, pick up, and displace downstream formerly deposited sediment fractions. This would result in a depositional mix of increasing proportions of older fractions that are incorporated into the more recent materials released along the fluid transit path.

As examples of “stop-and-go” transport effects are radiocarbon dates obtained for four of six Holocene samples obtained from core S-44. Four of these were found to be much older than ages attributed archaeologically by potsherds [6]. This age offset likely resulted from the fluvial sediment used for the radiocarbon analyses at this locality that had incorporated older reworked organic carbon material during transport to the site. These sediments are interpreted as having been eroded upstream and displaced over time by Nile flow on their way to the core S-44 site, unlike the sherds that were likely introduced locally and more directly concentrated into the channel’s older deposits. Two of the six radiocarbon-dated sediment samples, however, with materials obtained at core depths of ~14 m and ~6.5 m recorded more reasonable dates of ~7000 years B.P. and 3260 ± 90 years B.P., respectively. The latter younger date is the one most comparable to the archaeologically dated potsherd section at that depth (at “NK?” in Figure 5a).

4. Discussion

Sediment coring, recovering datable human materials, is one of the underlying reasons we proceeded with the present study: to encourage archaeologists to take cores at, and within, archaeological sites and record where and what possible dated anthropogenic materials are associated with sediment. Such additional closely spaced sampling and dating of smaller artifacts and associated sediments could perhaps provide further useful information to add to that collected at stages of initial exploration and perhaps also even to some settings having reached advanced levels of artifact excavation.

To date, there is strong evidence of human presence as of ~3600–3500 years B.P. based on findings in core S-44, and, from that time on, anthropogenic activity here appears to have occurred discontinuously. Thorough subsurface archaeological exploration of the north-central delta is still lacking; it has not yet been confirmed whether a temporary, periodically occupied, or more permanent settlement existed in the study area. The closest sites to S-44 known so far are Kom Nashwein and Tell Mikheizen, both about 15 km to the southwest (Figure 4). Both were visited by the Egypt Exploration Society Delta Surveys (IDs 263 and 266) and surface remains and artifacts were found to date to the Late Antique era; it is unclear if earlier occupation levels exist. Nor has it been established what range of human activities actually prevailed at, or in close proximity, to the S-44 site. The prime evidence for discontinuous activity remains the episodic concentrations of superposed core layers without potsherds at this one site. For example, no obvious evidence is found in the core’s Middle to Upper Holocene sequence, from ~7000 years B.P. to the base of the lower sherd level dated as Second Intermediate Period and early New Kingdom at ca. 3600–3500 years B.P. After an accumulation of the New Kingdom sherd sequence, the core again reveals an absence of anthropogenic material lasting from ~3200–2800 years B.P. until the Proto-Saitic/Saitic to Late Period (ca. 2700–2300 years B.P.), at a time gap between phases of obvious human activity lasting perhaps ~300 to 400 years. This was followed by a shorter span of only ~100 years, once again without apparent human activity, between the Late Period and Ptolemaic-Roman time (ca. 2300 to ~2200–1800 years B.P.). Additionally of note is the short core length of only 1.7 m near the core top that represents a relatively long period from ~1800 years ago to present and that remains without distinct

evidence of human activity. This latter youngest gap may have experienced substantial erosion of upper channel and marsh deposits, as well as the termination of Nile flow in the Sebennitic channel by about 1200 to 1000 years B.P. as has been suggested elsewhere [2,3].

Periodic absences of anthropogenic material at the times recorded above were initially viewed as little more than a possible discontinuous occupation by settlers moving periodically into and out of this area proximal to the channel site. During the past three decades, however, there has been a marked increase in paleoclimatic research that is providing insight on potential human presence and/or migration due to significant climate fluctuations. This work can now be reasonably applied to a broad area in the eastern Levantine Basin of the Mediterranean, including the study area and other localities examined in and beyond the delta (Table 1). This sector is in proximity to Mediterranean areas where the evolution of Nile flow through time may well have been modified by climatic influences emanating in the North Atlantic, and affecting sites to as far east as, and even beyond, the Eastern Mediterranean. Additionally significant are the monsoonal and ITCZ events triggered in highland areas of the Nile sources in northeastern Africa. These climatic factors substantially altered temperatures and rainfall intensities that, in turn, affected Nile flood levels and thus capable of playing a significant role in modifying the Upper Holocene archaeological history of Egypt and affected extensive Eastern Mediterranean and Levantine regions as recorded in [47–52].

Among the periods identified are several that have recorded wide-ranging effects, with some leading to marked decreased rainfall and increased number of aridity to serious drought phases (Table 1). Initially much, if not most, previous attention on the Nile delta evolution has been paid to the ~4200–4000 years B.P. event [45,46,53]. Of interest in the delta, for example, are those recorded at ca. 5000 years B.P., ca. 4200–4000 years B.P., ca. 3200–3000 years B.P., ca. 2800–2700 years B.P., ca. 2300–2200 years B.P., and periodically since 2000 years B.P. (Figure 5b–d). The two earlier phases cited above are not recorded at the S-44 site (Figure 5a) perhaps due to the subsequent Sebennitic channel's later initial date of diversion and flow to the study locality that may have begun after 4000 years B.P. Others, however, such as the one dated at ca. 3200–3000 years B.P., and younger ones are nevertheless identified at study core S-44 (Figure 5a), as well as at the core S-53 positioned ~35 km west of the study area along the southwestern margin of Burullus lagoon (Figure 5b), at core S-21 recovered at the northeastern delta coast near Port Fouad (Figure 5c), and at Lake Qarun in the Faiyum Basin (Figure 5d) about 250 km south of the Burullus coastal headland. It appears that the periods of potsherd absences indicated in core S-44 can be reasonably correlated time-wise with documented periodically intensified dry phases and droughts that affected an extensive region as recorded by the rapidly increasing number of paleoclimatic research studies (Table 1).

Clarification is needed as to why and how such periods of aridification seemingly would have induced a scenario of repeated absences of potsherd during long periods of time as identified herein. If the S-44 locality was positioned along a navigational channel, one could envision the importance of maintaining sufficient Nile flow connections between it and other natural channels and canals. These may well have been used at that time as regional byways for the nautical transport and distribution of goods and/or food products. When waterway levels were sufficiently high, either a levee or proximal channel margin could have served as a practical natural setting for repeated transport boat landings and departures, and thus used as a possible nautical trade and/or distribution center. Under conditions of sufficient water flow, medium and shallow draft boats possibly sailed to and from the S-44 site into the delta and even farther inland for active trade and exchange [54]. Additionally, in view of the site's proximity to the delta's coastal margin, it is also possible that goods could have been transferred to and from larger ships at the coast or moored offshore.

Table 1. Approximate dates of aridification phases recorded in Egypt's Nile delta and regions north, east, and south of it.

Location	Approximate Dates of Aridification (in Years B.P.)	References
Akkadian collapse and northeast Africa	4200–3900; 3200–3100	[51]
Mediterranean	4200	[55]
Eastern Mediterranean	3200	[49]
Eastern Mediterranean	3200–3000; 2900–2850	[50]
Eastern Mediterranean	4200; 3200–3100	[51]
Eastern Mediterranean	5500–5200; 4200–3900; 3200–2800; 2300; 1800; 1700	[56]
Eastern Mediterranean, Israel, and Egypt	5300–5000; 4500–3900; 3200–2800	[57]
Israel and Egypt	3200	[48]
Maryut Lake and northwest delta coast	Flow decreased to 3200 BP	[58]
Burullus lagoon region	3rd–7th century AD; 7th–9th century AD	[34,35]
Nile delta	4200–4000	[45,46,53]
Central delta	5800–5500; 4200–4000; 3400–3050	[59]
Saqqara necropolis	4100–3950	[60]
Faiyum depression	4800–4000; 3100–2800; After 2700	[43]
Faiyum depression	4200–4000; 3300–3100; 2500–2000; 1700–1500; 900–500	[61]
Faiyum depression	5700–5450; 4200; 3300–3100; 2800–2550; 400	[54]
Faiyum depression	6300–5600; 4200–4000; 3300–2800; 2500–2400; 1600–1500	[62]
Faiyum depression	5800–5400; 4200–4000; 3900–3000; 2300–2000; 1000–Present	[63]
Faiyum depression	5000; 4000 year BP is minimalized; 2700–2300	[64]
Lower Egypt	5350–5100; 4000	[65,66]
Nile downstream from Khartoum	3300	[67]

However, a fluctuating drying to arid climate leading to reduced rainfall and increased evaporitic conditions may well have led to a periodic diminished and insufficient Nile flow level, thus hindering nautical movement up and downstream channels and canals. Such fluctuating climatic conditions could periodically have also led to decreased agricultural production, with an insufficient food supply to support a population living and working in the area near the channel site, and thus hindering trade activities there as well.

5. Conclusions

The focus herein is on the paleogeographic and chronostratigraphic attributes of Upper Holocene sedimentary sequences without anthropogenic materials that are interbedded between archaeologically dated potsherd-rich layers in northern delta channel deposits. The prime questions relate specifically to when and why such sediment layers without pottery periodically accumulated along a subsidiary channel of the Sebennitic distributary. These deposits are denoted by time spans relative to thin double dashed black lines and circled numbers ① to ⑥ in Figure 5a–d. The oldest dated strata without potsherds or other anthropogenic materials in study core S-44 occurred during the long period (coded by numbers ⑥ and ⑤) from the late Middle Holocene (~7000 years B.P.) to the early part of the Upper Holocene (~3600 years B.P.), the latter identified as the New Kingdom. This was followed in the Upper Holocene by a time span without potsherds that included the second part of the Ramessid and some of the Third Intermediate periods (~3200 to ~2800 years B.P., ④), and then by a considerably shorter period of about 100 years without potsherds in the Ptolemaic period (~2300 to ~2200 years B.P., ③). Additional climatic aridification episodes also occurred after Ptolemaic-Roman times to the present as indicated by numbers ② and

① shown in Figure 5b–d. These latter youngest events are not clearly distinguished in the intensely eroded and much shorter 1.7 m length of the uppermost core section in S-44 (Figure 5a).

It is probable that the arid episodes identified here varied to some extent regionally with respect to both intensity and length of duration. In some instances, post-depositional effects such as erosion [68] and sediment compaction [27] could also have somewhat further modified apparent intensities and times of aridification. In some cases, serious drought events associated with more intense drying periods, in turn, may have seriously diminished the Nile's flow levels along its northward paths to and through the delta and its coastal margin. As suggested herein, such phases would have had a probable effect on limiting navigational frequencies, selecting alternate accessible nautical paths, and modifying local to regional anthropogenic trade activities. It is proposed that the cause-and-effect responses outlined herein could also be recorded at about the same times along some other channels and at their proximal associated archaeological sites in other Nile delta sectors.

Core analysis remains a geoarchaeological tool of prime value for identifying and interpreting some of the non-obvious yet significant anthropological and environmental factors that can be extracted from the study of subsurface sedimentary sequences. This approach provides a means to more comprehensively examine records of the past, including those that are subtle and potentially overlooked, obtained at both long-explored classic and more recently discovered archaeological sites.

Author Contributions: Conceptualization, J.-D.S. and E.L.-A.; data curation, J.-D.S. and T.U.; formal analysis, J.-D.S., T.U. and E.L.-A.; investigation, J.-D.S. and E.L.-A.; methodology, J.-D.S. and T.U.; project administration, J.-D.S.; software, T.U.; visualization, J.-D.S. and T.U.; writing—original draft, J.-D.S.; writing—review and editing, J.-D.S., T.U. and E.L.-A. All authors have read and agreed to the published version of the manuscript.

Funding: This research received no external funding.

Institutional Review Board Statement: Not applicable.

Informed Consent Statement: Not applicable.

Data Availability Statement: The digital elevation model of the TanDEM-X mission is shown with the permission of the German Aerospace Center (DLR), Germany, © DLR 2015–2020. The data were requested via the proposal DEM_HYDR1426.

Acknowledgments: We thank S. Wedl for her considerable assistance in manuscript preparation, and N. A. Ellis for an initial review of the manuscript, as well as the three journal reviewers for their constructive suggestions. We also thank Robert Schiestl (LMU Munich) for providing the SoE map sheets and Verena Stegmaier for her support in digitizing the SoE maps.

Conflicts of Interest: The authors declare no conflict of interest.

References

1. Herodotus; Grene, D. *The History*; University of Chicago Press: Chicago, IL, USA, 1987; 699p, ISBN 0-226-32772-8.
2. Sestini, G. Implications of climatic changes for the Nile Delta. In *Climatic Change and the Mediterranean*; Jeftic, L., Milliman, J.D., Sestini, G., Eds.; Arnold: London, UK, 1992; Volume 1, pp. 535–601.
3. United Nations Development Program (UNDP/UNESCO) Coastal Protection Studies. In *Arab Republic of Egypt: UNDP/EGY/73/063 Final Technical Report, United Nations Educational, Scientific and Cultural Organization*; United Nations Development Program: Paris, France, 1978; p. 438.
4. Said, R. *The Geological Evolution of the River Nile*; Springer: New York, NY, USA, 1981.
5. Toussoun, O. *Mémoire sur les Anciennes Branches du Nil: Époque Ancienne*; Impr. de l'Institut Français d'Archéologie Orientale: Le Caire, Egypt, 1922.
6. Stanley, D.J.; Arnold, D.; Warne, A.G. Oldest Pharaonic Site yet Discovered in the North-Central Nile Delta, Egypt. *Natl. Geogr. Res. Explor.* **1992**, *8*, 264–275.
7. Stanley, J.-D.; Warne, A.G.; Davis, H.R.; Bernasconi, M.P.; Chen, Z. Nile Delta. *Natl. Geogr. Res. Explor.* **1992**, *8*, 22–51.
8. Butzer, K.W. *Early Hydraulic Civilization in Egypt: A Study in Cultural Ecology*; Prehistoric Archeology and Ecology; The University of Chicago Press: Chicago, IL, USA, 1976; ISBN 978-0-226-08635-4.
9. Stanley, D.J.; Warne, A.G. Nile Delta: Recent Geological Evolution and Human Impact. *Science* **1993**, *260*, 628–634. [[CrossRef](#)]

10. Frihy, O.E.; Debes, E.A.; El Sayed, W.R. Processes reshaping the Nile delta promontories of Egypt: Pre- and post-protection. *Geomorphology* **2003**, *53*, 263–279. [[CrossRef](#)]
11. Arbouille, D.; Stanley, D.J. Late Quaternary evolution of the Burullus lagoon region, north-central Nile delta, Egypt. *Mar. Geol.* **1991**, *99*, 45–66. [[CrossRef](#)]
12. El-Asmar, H.M.; Hereher, M.E.; El Kafrawy, S.B. Surface area change detection of the Burullus Lagoon, North of the Nile Delta, Egypt, using water indices: A remote sensing approach. *Egypt. J. Remote Sens. Space Sci.* **2013**, *16*, 119–123. [[CrossRef](#)]
13. Frihy, O.E.; Loffy, M.F. Mineralogic evidence for the remnant Sebennitic promontory on the continental shelf off the central Nile delta. *Mar. Geol.* **1994**, *117*, 187–194. [[CrossRef](#)]
14. Frihy, O.; Debes, E. Beach and Nearshore Morphodynamics of the Central-Bulge of the Nile Delta Coast, Egypt. *Int. J. Environ. Prot.* **2011**, *1*, 33–46.
15. Frihy, O.E. Nile Delta shoreline changes: Aerial photographic study of a 28-year period. *J. Coast. Res.* **1988**, *4*, 597–606.
16. El Banna, M.M. Nature and human impact on Nile Delta coastal sand dunes, Egypt. *Environ. Earth Sci.* **2004**, *45*, 690–695. [[CrossRef](#)]
17. Hossen, H.; Negm, A. Change detection in the water bodies of Burullus Lake, Northern Nile Delta, Egypt, using RS/GIS. *Procedia Eng.* **2016**, *154*, 951–958. [[CrossRef](#)]
18. Gebremichael, E.; Sultan, M.; Becker, R.; El Bastawesy, M.; Cherif, O.; Emil, M. Assessing Land deformation and sea encroachment in the Nile Delta: A radar interferometric and inundation modeling approach. *J. Geophys. Res. Solid Earth* **2018**, *123*, 3208–3224. [[CrossRef](#)]
19. El Bastawesy, M.; Gebremichael, E.; Sultan, M.; Attwa, M.; Sahour, H. Tracing Holocene channels and landforms of the Nile Delta through integration of early elevation, geophysical, and sediment core data. *Holocene* **2020**, *30*, 1129–1141. [[CrossRef](#)]
20. Stanley, D.J.; McRea, J.E.; Waldron, J.C. Nile Delta drill core and sample database for 1985–1994: Mediterranean Basin (MEDIBA) Program. *Smithson. Contrib. Mar. Sci.* **1996**, *37*, 1–428. [[CrossRef](#)]
21. Butzer, K.W. Geoarchaeological implications of recent research in the Nile Delta. In *Egypt and the Levant: Interrelations from the 4th through the Early 3rd Millennium BCE*; Van den Brink, E.C.M., Levy, T.E., Eds.; Leicester University Press: London, UK.; New York, NY, USA, 2002; pp. 83–97.
22. Hereher, M.E. Vulnerability of the Nile Delta to sea level rise: An assessment using remote sensing. *Geomat. Nat. Hazards Risk* **2010**, *1*, 315–321. [[CrossRef](#)]
23. El-Hattab, M.M. Improving Coastal Vulnerability Index of the Nile Delta Coastal Zone, Egypt. *J. Earth Sci. Clim. Chang.* **2015**, *6*, 06. [[CrossRef](#)]
24. El-Geziry, T.M. On the vulnerability of the Egyptian Mediterranean Coast to the sea level rise. *Athens J. Sci.* **2020**, *7*, 195–206. [[CrossRef](#)]
25. Hasan, E.; Khan, S.I.; Hong, Y. Investigation of potential sea level rise impact on the Nile Delta, Egypt using digital elevation models. *Environ. Monit. Assess.* **2015**, *187*, 649. [[CrossRef](#)] [[PubMed](#)]
26. Stanley, J.-D.; Clemente, P.L. Increased land subsidence and sea-level rise are submerging Egypt's Nile Delta coastal margin. *GSA Today* **2017**, 4–11. [[CrossRef](#)]
27. Stanley, J.-D.; Corwin, K.A. Measuring strata thicknesses in cores to assess recent sediment compaction and subsidence of Egypt's Nile Delta coastal margin. *J. Coast. Res.* **2013**, *288*, 657–670. [[CrossRef](#)]
28. Korrat, I.; El Agami, N.; Hussein, H.; El-Gabry, M. Seismotectonics of the passive continental margin of Egypt. *J. Afr. Earth Sci.* **2005**, *41*, 145–150. [[CrossRef](#)]
29. Mohamed, A.E.-E.A.; Elhadidy, M.; Deif, A.; Elenean, K.A. Seismic hazard studies in Egypt. *NRIAG J. Astron. Geophys.* **2012**, *1*, 119–140. [[CrossRef](#)]
30. Kebeasy, R.M. Seismicity. In *The Geology of Egypt: Rotterdam*; Said, R., Ed.; A.A. Balkema: Rotterdam, The Netherlands, 1990; pp. 51–59.
31. Ullmann, T.; Lange-Athinodorou, E.; Göbel, A.; Büdel, C.; Baumhauer, R. Preliminary results on the paleo-landscape of Tell Basta/Bubastis (eastern Nile delta): An integrated approach combining GIS-Based spatial analysis, geophysical and archaeological investigations. *Quat. Int.* **2019**, *511*, 185–199. [[CrossRef](#)]
32. Gruber, S.; Peckham, S. Chapter 7 Land-Surface parameters and objects in hydrology. In *Developments in Soil Science*; Hengl, T., Reuter, H.I., Eds.; Geomorphometry; Elsevier: Amsterdam, The Netherlands, 2009; Volume 33, pp. 171–194.
33. Wang, L.; Liu, H. An efficient method for identifying and filling surface depressions in digital elevation models for hydrologic analysis and modelling. *Int. J. Geogr. Inf. Sci.* **2006**, *20*, 193–213. [[CrossRef](#)]
34. Wilson, P. Landscapes of the Bashmur: Settlements and monasteries in the northern Egyptian Delta from the seventh to the ninth century. In *The Nile: Natural and Cultural Landscape in Egypt*; Willems, H., Dahms, J.-M., Eds.; Transcript Verlag: Bielefeld, Germany, 2017; pp. 345–368, ISBN 978-3-8394-3615-8.
35. Wilson, P. Human and deltaic environments in northern Egypt in late antiquity. *Environ. Soc. Long Late Antiq.* **2019**, 224–244. [[CrossRef](#)]
36. Tallet, P. Les Papyrus de La Mer Rouge I: Le “Journal de Merer” (Papyrus Jarf A et B). *Mémoires Publiés Par Les Membres de l'Inst. Français D'archéologie Orient.* **2017**, 136, 176.
37. Dumont, H.J.; El-Shabrawy, G.M. Lake Borullus of the Nile Delta: A short history and an uncertain future. *AMBIO A J. Hum. Environ.* **2007**, *36*, 677–682. [[CrossRef](#)]

38. Kafrawy, S.; Khalafallah, A.; Omar, M.; Khalil, M.; Yehia, A.; Allam, M. An integrated field and remote sensing approach for water quality mapping of Lake Burullus, Egypt. *Int. J. Environ. Sci. Eng.* **2016**, *6*, 17–20.
39. Zibelius, K. *Ägyptische Siedlungen Nach Texten Des Alten Reiches*; Beihefte zum Tübinger Atlas des Vorderen Orients. Reihe B (Geisteswissenschaften) 19; Reichert Verlage: Wiesbaden, Germany, 1978; p. 312.
40. Spencer, J. *The Delta Survey, 2009–2015*; Egypt Exploration Society, Excavation Memoir 112; Egypt Exploration Society: London, UK, 2016.
41. Bernhardt, C.E.; Horton, B.; Stanley, J.-D. Nile Delta vegetation response to Holocene climate variability. *Geology* **2012**, *40*, 615–618. [[CrossRef](#)]
42. Krom, M.; Stanley, J.-D.; Cliff, R.; Woodward, J. Nile River sediment fluctuations over the past 7000 yr and their key role in sapropel development. *Geology* **2002**, *30*, 71–74. [[CrossRef](#)]
43. Hassan, F. Holocene lakes and prehistoric settlements of the Western Faiyum, Egypt. *J. Archaeol. Sci.* **1986**, *13*, 483–501. [[CrossRef](#)]
44. Stanley, J.-D. Dating modern deltas: Progress, problems, and prognostics. *Annu. Rev. Earth Planet. Sci.* **2001**, *29*, 257–294. [[CrossRef](#)]
45. Marriner, N.; Flaux, C.; Morhange, C.; Kaniewski, D. Nile Delta's sinking past: Quantifiable links with Holocene compaction and climate-driven changes in sediment supply? *Geology* **2012**, *40*, 1083–1086. [[CrossRef](#)]
46. Stanley, J.-D. Egypt's Nile Delta in late 4000 years BP: Altered flood levels and sedimentation, with archaeological implications. *J. Coast. Res.* **2019**, *35*, 1036. [[CrossRef](#)]
47. Kaniewski, D.; Van Campo, E.; Guiot, J.; Le Burel, S.; Otto, T.; Baeteman, C. Environmental roots of the late Bronze Age Crisis. *PLoS ONE* **2013**, *8*, e71004. [[CrossRef](#)]
48. Kaniewski, D.; Marriner, N.; Bretschneider, J.; Jans, G.; Morhange, C.; Cheddadi, R.; Otto, T.; Luce, F.; Van Campo, E. 300-year drought frames Late Bronze Age to Early Iron Age transition in the Near East: New palaeoecological data from Cyprus and Syria. *Reg. Environ. Chang.* **2019**, *19*, 2287–2297. [[CrossRef](#)]
49. Kaniewski, D.; Guiot, J.; Van Campo, E. Drought and societal collapse 3200 years ago in the Eastern Mediterranean: A review. *Wiley Interdiscip. Rev. Clim. Chang.* **2015**, *6*, 369–382. [[CrossRef](#)]
50. Kaniewski, D.; Van Campo, E. 3.2 ka BP Megadrought and the Late Bronze Age Collapse. In *3.2 ka BP Megadrought and the Late Bronze Age Collapse*; Oxford University Press (OUP): Oxford, UK, 2017; Volume 1.
51. Weiss, H. Megadrought, collapse and causality, A note on chronology. In *Megadrought and Collapse from Early Agriculture to Angkor*; Weiss, H., Ed.; Oxford University Press, Sheridan Books: Oxford, UK, 2017; pp. 1–31, ISBN 978-0-19-932919-9.
52. Weiss, H. 4.2 ka BP Megadrought and the Akkadian Collapse. In *Megadrought and Collapse from Early Agriculture to Angkor*; Weiss, H., Ed.; Oxford University Press, Sheridan Books: Oxford, UK, 2017; Chapter 3; pp. 93–159, ISBN 978-0-19-932919-9.
53. Marriner, N.; Flaux, C.; Morhange, C.; Stanley, J.-D. Tracking Nile Delta vulnerability to Holocene change. *PLoS ONE* **2013**, *8*, e69195. [[CrossRef](#)]
54. Macklin, M.G.; Toonen, W.H.; Woodward, J.; Williams, M.A.; Flaux, C.; Marriner, N.; Nicoll, K.; Verstraeten, G.; Spencer, N.; Welsby, D. A new model of river dynamics, hydroclimatic change and human settlement in the Nile Valley derived from meta-analysis of the Holocene fluvial archive. *Quat. Sci. Rev.* **2015**, *130*, 109–123. [[CrossRef](#)]
55. Bini, M.; Zanchetta, G.; Perşoiu, A.; Cartier, R.; Català, A.; Cacho, I.; Dean, J.R.; Di Rita, F.; Drysdale, R.N.; Finnè, M.; et al. The 4.2 ka BP Event in the Mediterranean region: An overview. *Clim. Past* **2019**, *15*, 555–577. [[CrossRef](#)]
56. Kaniewski, D.; Marriner, N.; Cheddadi, R.; Fischer, P.M.; Otto, T.; Luce, F.; Van Campo, E. Climate change and social unrest: A 6,000-year chronicle from the eastern Mediterranean. *Geophys. Res. Lett.* **2020**, *47*, 7. [[CrossRef](#)]
57. Roberts, N.; Eastwood, W.J.; Kuzucuoglu, C.; Fiorentino, G.; Caracuta, V. Climatic, vegetation and cultural change in the eastern Mediterranean during the mid-Holocene environmental transition. *Holocene* **2011**, *21*, 147–162. [[CrossRef](#)]
58. Flaux, C.; Elassal, M.; Marriner, N.; Morhange, C.; Rouchy, J.-M.; Soulié-Märsche, I.; Torab, M. Environmental changes in the Maryut lagoon (northwestern Nile delta) during the last ~2000 years. *J. Archaeol. Sci.* **2012**, *39*, 3493–3504. [[CrossRef](#)]
59. Zhao, X.; Thomas, I.; Salem, A.; Alassal, S.E.; Liu, Y.; Sun, Q.; Chen, J.; Ma, F.; Finlayson, B.; Chen, Z. Holocene climate change and its influence on early agriculture in the Nile Delta, Egypt. *Palaeogeogr. Palaeoclim. Palaeoecol.* **2020**, *547*, 109702. [[CrossRef](#)]
60. Welc, F.; Marks, L. Climate change at the end of the Old Kingdom in Egypt around 4200 BP: New geoarchaeological evidence. *Quat. Int.* **2014**, *324*, 124–133. [[CrossRef](#)]
61. Baioumy, H.M.; Kayanne, H.; Tada, R. Reconstruction of lake-level and climate changes in Lake Qarun, Egypt, during the last 7000 years. *J. Great Lakes Res.* **2010**, *36*, 318–327. [[CrossRef](#)]
62. Zalat, A.A.; Marks, L.; Welc, F.; Salem, A.; Nitychoruk, J.; Chen, Z.; Majecka, A.; Szymanek, M.; Chodyka, M.; Tołoczko-Pasek, A.; et al. Diatom stratigraphy of FA-1 core, Qarun Lake, records of Holocene environmental and climatic change in Faiyum Oasis, Egypt. *Stud. Quat.* **2017**, *34*, 61–69. [[CrossRef](#)]
63. Zhao, X.; Liu, Y.; Salem, A.; Marks, L.; Welc, F.; Sun, Q.; Jiang, J.; Chen, J.; Chen, Z. Migration of the Intertropical Convergence Zone in North Africa during the Holocene: Evidence from variations in quartz grain roundness in the lower Nile valley, Egypt. *Quat. Int.* **2017**, *449*, 22–28. [[CrossRef](#)]
64. Sun, Q.; Liu, Y.; Salem, A.; Marks, L.; Welc, F.; Ma, F.; Zhang, W.; Chen, J.; Jiang, J.; Chen, Z. Climate-induced discharge variations of the Nile during the Holocene: Evidence from the sediment provenance of Faiyum Basin, north Egypt. *Glob. Planet. Chang.* **2019**, *172*, 200–210. [[CrossRef](#)]

65. Pennington, B.; Sturt, F.; Wilson, P.; Rowland, J.; Brown, A. The fluvial evolution of the Holocene Nile Delta. *Quat. Sci. Rev.* **2017**, *170*, 212–231. [[CrossRef](#)]
66. Pennington, B.T.; Wilson, P.; Sturt, F.; Brown, A.G. Landscape change in the Nile Delta during the fourth millennium BC: A new perspective on the Egyptian Predynastic and Protodynastic periods. *World Archaeol.* **2020**, *52*, 550–565. [[CrossRef](#)]
67. Woodward, J.; Macklin, M.; Fielding, L.; Millar, I.; Spencer, N.; Welsby, D.; Williams, M. Shifting sediment sources in the world's longest river: A strontium isotope record for the Holocene Nile. *Quat. Sci. Rev.* **2015**, *130*, 124–140. [[CrossRef](#)]
68. Goodfriend, G.A.; Stanley, D.J. Reworking and discontinuities in Holocene sedimentation in the Nile Delta: Documentation from amino acid racemization and stable isotopes in mollusk shells. *Mar. Geol.* **1996**, *129*, 271–283. [[CrossRef](#)]